Nonlinear Vibration of Rotating Corotational Two-Dimensional Beams With Large Displacement

Zihan Shen, Benjamin Chouvion, Fabrice Thouverez, Aline Beley, Jean-Daniel Beley

Zihan Shen
Ecole Centrale de Lyon,
LTDS UMR 5513,
Ecully 69130, France;
ANSYS France,
Villeurbanne 69100, France
e-mail: zihan.shen@doctorant.ec-lyon.fr

Benjamin Chouvion
Ecole Centrale de Lyon,
LTDS UMR 5513,
Ecully 69130, France

Fabrice Thouverez
Ecole Centrale de Lyon,
LTDS UMR 5513,
Ecully 69130, France

Aline Beley
ANSYS France,
Villeurbanne 69100, France

Jean-Daniel Beley
ANSYS France,
Villeurbanne 69100, France

Nonlinear Vibration of Rotating Corotational Two-Dimensional Beams With Large Displacement

In this paper, the nonlinear vibrations of rotating beams with large displacements are investigated by the use of the co-rotational (C-R) finite element method. In the C-R approach, the full motion is decomposed into a rigid body part and a pure deformational part by introducing a local coordinate system attached to the element. The originality we propose in this study is to derive its formulation in a rotating reference frame and include both centrifugal and gyroscopic effects. The nonlinear governing equations are obtained from Lagrange's equations using a consistent expression for the kinetic energy. With this formulation, the spin-stiffening effect from geometrical nonlinearities due to large displacements is accurately handled. The proposed approach is then applied to several types of mechanical analysis (static large deformation, modal analysis at different spin speeds, and transient analysis after an impulsive force) to verify its accuracy and demonstrate its efficiency.

1 Introduction

Flexible beams are widely used in many applications of turbomachinery, for instance, in turbine vane [1], or helicopter blade and wind propellers [2,3]. In recent years, the turbomachines manufacturers went toward even faster, larger, and lighter structure designs. Thus, these structures do not only have greater centrifugal forces and Coriolis effects but also often undergo larger displacements. This may explain why the study of rotating beams dynamics has drawn a lot of attention in the literature. However, the number of studies in which both geometrical nonlinearity and centrifugal force effects are taken into consideration is limited. The first geometrically nonlinear finite element rotating beam model was proposed by Bauchau and Hong [3]. Much later, the *p*-version finite element method was devised to investigate the nonlinear vibration of rotating beam [2]. The spectral finite element method was also introduced [4] to study the nonlinear vibration from impulse excitation. Subsequently, the nonlinear normal modes and harmonic balance methods were applied to study nonlinear forced vibration of rotating beams [1,5]. However, all the aforementioned rotating beam models are dedicated and limited to moderate amplitude vibration. Recently, the geometrical nonlinear co-rotational formulation has demonstrated its great efficiency in very large displacement dynamic analysis, with the particularity to use the formulation of a consistent mass matrix instead of a constant mass matrix [6]. The consistent mass matrix allows taking the rigid body motion into consideration. To the authors' knowledge, the full consistent geometrical nonlinear co-rotational formulations of rotating beams are not reported, to this day, in the literature, and this is the main consideration of this paper.

The C-R approach has been widely used to solve static problems with very large displacements [7,8]. Its key concept is to separate the full global motion of the structure into a rigid body motion and a pure deformational part, via the introduction of local attached co-rotated frames. Furthermore, by extracting the pure deformational part, the strain energy of the structure can be evaluated directly using a small strain hypothesis. It means that several existing linear finite element models can be re-used with the C-R approach. The fact that the C-R approach is element independent is a well-known property. An overview of the C-R approach can be found in Ref. [9].

Two main contributions are developed in the current study. The first one is that we consider both centrifugal and gyroscopic effects in the consistent C-R dynamic formulation in order to introduce the dynamic C-R formulation into turbomachinery modeling. The second main objective of the current work is to formulate the equations of motion of the structure in its rotating reference frame. The procedure employed is to derive the inertia nodal forces and deformational nodal forces from Lagrange's equations using exact expression of kinetic and strain energies. The analytical mass, Coriolis, tangent dynamic stiffness, and tangent elastic stiffness matrices are also derived by differentiating the inertia and deformational nodal forces. To validate the proposed formulation and demonstrate its time efficiency, different simulations are performed and compared with literature or commercial finite element software (ANSYS). We investigate the static large deformation due to centrifugal force, the free vibration of a rotating beam around a prestressed deformation, very large transient vibrations, and the effect of an impulsive force on a rotating beam. It is expected that the proposed approach offers substantial computation time saving compared to ANSYS by using a smaller number of elements.

2 Beam Kinemtaics

In this paper, the C-R finite element method is applied to the rotating planar beam shown in Fig. 1. The flexible beam is attached to a rigid hub of radius a, and is rotating with a constant spin speed Ω. The beam has an uniform cross section and is made of elastic isotropic material. The length of the beam is L, its width b, and thickness h. The fixed reference frame (Galilean reference frame) is indicated by $(\bar{\mathbf{X}}, \bar{\mathbf{Y}}, \bar{\mathbf{Z}})$. The rotating reference frame named ($\mathbf{X}$, $\mathbf{Y}$, $\mathbf{Z}$) is attached to the beam. Any vector $\mathbf{V}_r$ defined in

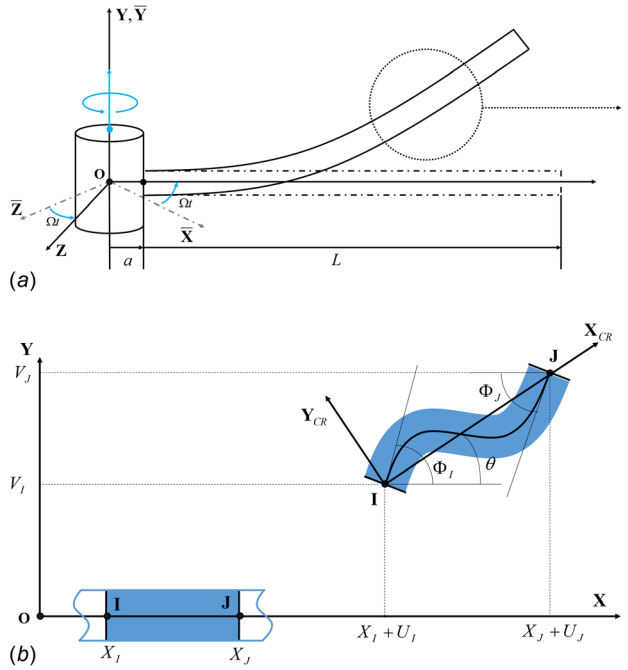

Fig. 1 Kinematics of rotating deformed beam: (*a*) global kinematics and (*b*) local kinematics

the rotating reference frame can be expressed in the fixed reference frame (then noted $\mathbf{V}_f$) by using the rotation matrix $\mathbf{T}_r^f$

$$\mathbf{V}_f = \begin{bmatrix} \cos(\Omega t) & 0 & \sin(\Omega t) \\ 0 & 1 & 0 \\ -\sin(\Omega t) & 0 & \cos(\Omega t) \end{bmatrix} \mathbf{V}_r = \mathbf{T}_r^f \mathbf{V}_r \tag{1}$$

The subscripts f and r represent, respectively, the fixed and rotating reference frames. The origin of $(\bar{\mathbf{X}}, \bar{\mathbf{Y}}, \bar{\mathbf{Z}})$ coincides with the origin of $(\mathbf{X}, \mathbf{Y}, \mathbf{Z})$ and is noted O in Fig. 1. The beam axial axis in the initial configuration coincides with the X-axis. If one arbitrary discretized C-R beam element is considered, its displacement in the rotating reference frame is defined with

$$\mathbf{q} = \begin{bmatrix} U_I & V_I & \Phi_I & U_J & V_J & \Phi_J \end{bmatrix}^{\mathrm{T}} \tag{2}$$

where U_i, V_I, and Φ_i (i being I or J) are, respectively, the nodal axial displacement, the nodal transversal displacement and the nodal cross section orientation. In the C-R formulation, there are different ways in which local co-rotated frames can be defined [7,10]. It can, for example, be the secant or the tangential co-rotated frame. Depending on the beams properties, an appropriate co-rotated frame can give a solution which converges to the reference solution obtained from total-Lagrange formulations [8]. The local kinematic of a rotating beam using a secant co-rotated frame $(\mathbf{X}_{\mathrm{CR}}, \mathbf{Y}_{\mathrm{CR}})$ is illustrated in Fig. 1. The co-rotational axial axis $\mathbf{X}_{\mathrm{CR}}$ is defined by connecting the two centers of the initial and final cross section of the beam element in the current configuration. The orientation of $\mathbf{X}_{\mathrm{CR}}$ can be parametrized by θ. The co-rotational lateral axis $\mathbf{Y}_{\mathrm{CR}}$ is simply defined as perpendicular to $\mathbf{X}_{\mathrm{CR}}$. The full global displacement of a beam element is then defined with two different set of parameters: 1. Rigid body motion: $[U_I, V_I]$ and θ; 2. Pure deformational motion: $\bar{\mathbf{q}} = \begin{bmatrix} \bar{u} & \bar{\Phi}_I & \bar{\Phi}_J \end{bmatrix}^{\mathrm{T}}$. The local nodal rotations $\bar{\Phi}_I$ and $\bar{\Phi}_J$ (at end I and J) with respect to the co-rotated reference are defined as

$$\bar{\Phi}_I = \Phi_I - \theta \qquad \bar{\Phi}_J = \Phi_J - \theta \tag{3}$$

The local axial displacement $\bar{u}$ is the difference between the current length L_n and the initial length L_0 of beam. In order to achieve a better numerical conditioning, $\bar{u}$ is expressed as

$$\bar{u} = \frac{L_n^2 - L_0^2}{L_n + L_0} \tag{4}$$

L_n and L_0 in Eq. (4) can be expressed with the nodal coordinates and nodal displacements

$$\begin{aligned} L_0 &= \sqrt{(Y_J - Y_I)^2 + (X_J - X_I)^2} \\ L_n &= \sqrt{(V_J - V_I + Y_J - Y_I)^2 + (U_J - U_I + X_J - X_I)^2} \end{aligned} \tag{5}$$

In order not to be limited on the range of possible nodal rotation of the element (Eq. (3)), the local nodal rotations can also be calculated with

$$\begin{aligned} \bar{\Phi}_I &= \arctan\left(\frac{\sin\Phi_I\cos\theta - \cos\Phi_I\sin\theta}{\cos\Phi_I\cos\theta + \sin\Phi_I\sin\theta}\right) \\ \bar{\Phi}_J &= \arctan\left(\frac{\sin\Phi_J\cos\theta - \cos\Phi_J\sin\theta}{\cos\Phi_J\cos\theta + \sin\Phi_J\sin\theta}\right) \end{aligned} \tag{6}$$

In this way, the range of θ is extended from $[-\pi/2, \pi/2]$ to $[-\pi, \pi]$. In Eq. (6), the trigonometric functions $\sin\theta$ and $\cos\theta$, defining the orientation of the co-rotated local reference frame, can be written as

$$\sin\theta = \frac{V_J - V_I + Y_J - Y_I}{L_n} \qquad \cos\theta = \frac{U_J - U_I + X_J - X_I}{L_n} \tag{7}$$

Finally, the relationship between infinitesimal local nodal displacements and global nodal displacements can be expressed by differentiating Eqs. (3)–(7) as $\delta\bar{\mathbf{q}} = \mathbf{B}\delta\mathbf{q}$ and where the strain matrix $\mathbf{B}$ is

$$\mathbf{B} = \begin{bmatrix} \mathbf{b}_1 \\ \mathbf{b}_2 \\ \mathbf{b}_3 \end{bmatrix} = \frac{1}{L_n} \begin{bmatrix} -L_n\cos\theta & -L_n\sin\theta & 0 & L_n\cos\theta & L_n\sin\theta & 0 \\ -\sin\theta & \cos\theta & L_n & \sin\theta & -\cos\theta & 0 \\ -\sin\theta & \cos\theta & 0 & \sin\theta & -\cos\theta & L_n \end{bmatrix} \tag{8}$$

The equations in Eqs. (3)–(12) are standard C-R derivations, which can be found in Refs. [6] and [11]. Some other important differentiation relationships can also be formulated using the aforementioned kinematic formulation (see Appendix A).

3 Beam Statics

In the C-R formulation, the local displacements field in the co-rotated reference is interpolated by conventional shape functions. Those shape functions depend on the type of element on which the C-R process is applied. In this work, Euler–Bernoulli beam elements are used. Hence, the local axial displacement u, the local transverse displacement v, and the local rotation ϕ in the $(\mathbf{X}_{\mathrm{CR}}, \mathbf{Y}_{\mathrm{CR}})$ frame are given by

$$u = \frac{x}{L_0}\bar{u} \qquad v = N_1\bar{\Phi}_I + N_2\bar{\Phi}_J \qquad \phi = N_3\bar{\Phi}_I + N_4\bar{\Phi}_J \tag{9}$$

where N_1, N_2, N_3, and N_4 are classical cubic Hermitian shape functions of Euler–Bernoulli beam elements. The local strain fields according to Euler–Bernoulli hypothesis are given by

$$\begin{aligned} \varepsilon &= u' = \frac{\bar{u}}{L_0} \\ \kappa &= v'' = \phi' = \left(6x/L_0^2 - 4/L_0\right)\bar{\Phi}_I + \left(6x/L_0^2 - 2/L_0\right)\bar{\Phi}_J \end{aligned} \tag{10}$$

The strain energy of an element is given by

$$E_s = \int_0^{L_0} \left(\frac{EA}{2}\varepsilon^2 + \frac{EI_z}{2}\kappa^2\right) dx \tag{11}$$

where EA and EI_z are, respectively, the axial and flexural rigidity of the beam. The local linear stiffness matrix is obtained as

$$\bar{\mathbf{K}} = \text{Hessian}(E_s, \bar{\mathbf{q}}) = \begin{bmatrix} \frac{\text{EA}}{L_0} & 0 & 0 \\ 0 & \frac{4EI_z}{L_0} & \frac{2EI_z}{L_0} \\ 0 & \frac{2EI_z}{L_0} & \frac{4EI_z}{L_0} \end{bmatrix} \tag{12}$$

The local axial force $\bar{N}$ and local end moments $\bar{M}_I$ and $\bar{M}_J$ of the beam are obtained with Eq. (12) and the local deformational vector $\bar{\mathbf{q}}$, the corresponding local elemental internal elastic force vector can be given as $\bar{\mathbf{f}}_E = \begin{bmatrix} \bar{N} & \bar{M}_I & \bar{M}_J \end{bmatrix}^{\mathrm{T}} = \bar{\mathbf{K}}\bar{\mathbf{q}}$. Furthermore, as the virtual elastic force work is equivalent in both global frame and local co-rotated reference frame, we have the expression

$$\delta E_s = \delta \mathbf{q}^{\mathrm{T}} \mathbf{f}_E = \delta \bar{\mathbf{q}}^{\mathrm{T}} \bar{\mathbf{f}}_E \tag{13}$$

Applying Eq. (8) in Eq. (13) gives the expression of the global internal elastic force vector $\mathbf{f}_E$ as

$$\mathbf{f}_E = \mathbf{B}^{\mathrm{T}} \bar{\mathbf{f}}_E = \mathbf{B}^{\mathrm{T}} \bar{\mathbf{K}} \bar{\mathbf{q}} \tag{14}$$

Finally, it is possible to formulate the expression of the global tangent elastic matrix $\mathbf{K}_e$ by differentiating $\mathbf{f}_E$ with respect to $\mathbf{q}$ and applying the differential relation in Appendix A

$$\mathbf{K}_e = \frac{\partial \mathbf{f}_e}{\partial \mathbf{q}} = \mathbf{B}^{\mathrm{T}} \bar{\mathbf{K}} \mathbf{B} + \mathbf{K}_N + \mathbf{K}_M \tag{15}$$

where the geometric stiffness for local axial force $\mathbf{K}_N$ and the geometric stiffness for local end moments $\mathbf{K}_M$ are given by

$$\mathbf{K}_N = \frac{\bar{N}}{L_n} \begin{bmatrix} \sin^2\theta & -\frac{\sin 2\theta}{2} & 0 & \sin^2\theta & \frac{\sin 2\theta}{2} & 0 \\ & \cos^2\theta & 0 & \frac{\sin 2\theta}{2} & -\cos^2\theta & 0 \\ & & 0 & 0 & 0 & 0 \\ & & & \sin^2\theta & -\frac{\sin 2\theta}{2} & 0 \\ & & & & \cos^2\theta & 0 \\ \text{Sym.} & & & & & 0 \end{bmatrix}$$

$$\mathbf{K}_M = \frac{\bar{M}_I + \bar{M}_J}{L_n^2} \begin{bmatrix} -\sin 2\theta & \cos 2\theta & 0 & \sin 2\theta & -\cos 2\theta & 0 \\ & \sin 2\theta & 0 & -\cos 2\theta & -\sin 2\theta & 0 \\ & & 0 & 0 & 0 & 0 \\ & & & -\sin 2\theta & \cos 2\theta & 0 \\ & & & & \sin 2\theta & 0 \\ \text{Sym.} & & & & & 0 \end{bmatrix} \tag{16}$$

4 Beam Dynamics

The position vector of an arbitrary material point P with the coordinates (x, y) in the element with respect to the rotating reference frame is given by (see Fig. 1)

$$\begin{aligned} \mathbf{OP}_r = {} & (X_I + U_I)\mathbf{X} + (Y_I + V_I)\mathbf{Y} + [x + u(x) - y\phi(x)] \\ & \mathbf{X}_{\text{CR}} + [v(x) + y]\mathbf{Y}_{\text{CR}} \end{aligned} \tag{17}$$

where

$$\mathbf{X}_{\text{CR}} = \cos\theta\mathbf{X} + \sin\theta\mathbf{Y} \quad \mathbf{Y}_{\text{CR}} = -\sin\theta\mathbf{X} + \cos\theta\mathbf{Y} \tag{18}$$

The position of the material point P under constant spin speed with respect to the fixed reference frame is simply expressed by using the rotation matrix $\mathbf{T}_r^f$ (see Eq. (1)) as $\mathbf{OP}_f = \mathbf{T}_r^f \mathbf{OP}_r$ Hence, the exact expression of the kinetic energy E_c for the beam element is given by

$$E_c = \frac{1}{2}\rho \int \left(\dot{\mathbf{OP}}_f^{\mathrm{T}} \dot{\mathbf{OP}}_f \right) dV \tag{19}$$

The material point's velocity vector $\dot{\mathbf{OP}}_f$ is function of the time-derivatives $\dot{\theta}$, $\dot{\tilde{\Phi}}_I$, and $\dot{\tilde{\Phi}}_J$, which can all directly be expressed as function of $\dot{\mathbf{q}}$. The kinetic energy, then function of $\mathbf{q}$, $\dot{\mathbf{q}}$, and $\bar{\mathbf{q}}$, is calculated by analytically integrating Eq. (19) in which all the second-order terms are kept, unlike other C-R formulations [6,12]. The kinetic energy takes the following form:

$$E_c = \frac{1}{2}\dot{\mathbf{q}}^{\mathrm{T}}\mathbf{M}\dot{\mathbf{q}} + \frac{1}{2}\mathbf{q}^{\mathrm{T}}\mathbf{K}_\Omega\mathbf{q} + \mathbf{F}_\Omega^{\mathrm{T}}\mathbf{q} + E_{NL} + E_{\text{cte}} \tag{20}$$

It contains five terms classified in different orders of $\dot{\mathbf{q}}$ and $\mathbf{q}$. Full derivation of each of these terms is given in Appendix A. For each term, the Lagrange's equation is applied to calculate the internal inertial force vector

$$\mathbf{f}_I^{(i)} = \frac{\mathrm{d}}{\mathrm{d}t}\left(\frac{\partial E_c^{(i)}}{\partial \dot{\mathbf{q}}} \right) - \frac{\partial E_c^{(i)}}{\partial \mathbf{q}} \tag{21}$$

The mass matrix $\mathbf{M}_d$, the gyroscopic matrix $\mathbf{C}_d$, and the tangent stiffness matrix $\mathbf{M}_d$, corresponding to the different terms of the kinetic energy, are also derived analytically for a rotating beam element with very large displacement and given by

$$\mathbf{M}_d^{(i)} = \frac{\partial \mathbf{f}_I^{(i)}}{\partial \ddot{\mathbf{q}}} \qquad \mathbf{C}_d^{(i)} = \frac{\partial \mathbf{f}_I^{(i)}}{\partial \dot{\mathbf{q}}} \qquad \mathbf{K}_d^{(i)} = \frac{\partial \mathbf{f}_I^{(i)}}{\partial \mathbf{q}} \tag{22}$$

Finally, the nonlinear equation of motion for the rotating C-R beam element with applied load vector $\mathbf{p}$ writes as

$$\mathbf{f}_I(\ddot{\mathbf{q}}, \dot{\mathbf{q}}, \mathbf{q}) + \mathbf{f}_E(\mathbf{q}) = \mathbf{p} \tag{23}$$

And $\mathbf{f}_I = \sum_{i=1}^{5} \mathbf{f}_I^{(i)}$. The corresponding tangent matrices for the full equation of motion can be formulated as

$$\tilde{\mathbf{M}} = \sum_{i=1}^{5} \mathbf{M}_d^{(i)} \qquad \tilde{\mathbf{C}} = \sum_{i=1}^{5} \mathbf{C}_d^{(i)} \qquad \tilde{\mathbf{K}} = \mathbf{K}_e + \sum_{i=1}^{5} \mathbf{K}_d^{(i)} \tag{24}$$

In the case of free vibration, the equations of motion can be simply formulated as

$$\tilde{\mathbf{M}}\ddot{\mathbf{q}} + \tilde{\mathbf{C}}\dot{\mathbf{q}} + \tilde{\mathbf{K}}\mathbf{q} = 0 \tag{25}$$

5 Numerical Application

In this section, several examples are presented to test the static and dynamic behavior of the proposed rotating C-R beam formulation. The equations of motion (23) are solved using implicit time-stepping algorithm [12]. A damping matrix equal to 10^{-4} times the linear elastic stiffness matrix is used. Characteristics of the beam used in the following simulations are given in Table 1.

Table 1 Properties of the simulated beam

L (m)	b (m)	h (m)	ρ (kg/m^3)	E (Gpa)
10	0.3	0.6	7850	210

The beam has a rectangular cross section (width b and thickness h).

6 Static Large Deformation Analysis

In order to demonstrate the behavior of the element in highly nonlinear cases, we simulate the bending of the beam in a rotating reference frame. A bending moment M is applied at the free end of the beam around the Z-axis. In classical beam theory, when the spin speed is null, the curvature after bending will be uniform for the whole beam due to $EI_z\kappa = M$. Thus, the uniform straight beam will be bent into a full circle under the critical moment $M_{\text{cr}} = 2\pi EI_z/L_0$ [13,14].

The beam is discretized into 5 elements and its deformation is plotted in Fig. 2(*a*) for five different values ($0.2M_{\text{cr}}$, $0.4M_{\text{cr}}$, $0.6M_{\text{cr}}$, $0.8M_{\text{cr}}$, and M_{cr}) of applied moments. With the proposed C-R element, the final solution can be achieved by directly applying the full M_{cr}. As shown, the rotation angle of the free end is exactly 2π at the final configuration. A similar numerical application using co-rotational formulation was reported by Crisfield [15]. The main difference with the current approach lies in the order of interpolation of the shape functions (linear in Ref. [15] and cubic here). With the absolute-nodal-coordinate-based beam element proposed by Omar and Shabana [16], the minimum number of elements was 16 to achieve a full circle.

When the spin speed is nonzero, the internal centrifugal force can also eventually lead to large static deformations. In the particular case of constant spin speed and a static analysis, the equations of motion for large deformation become

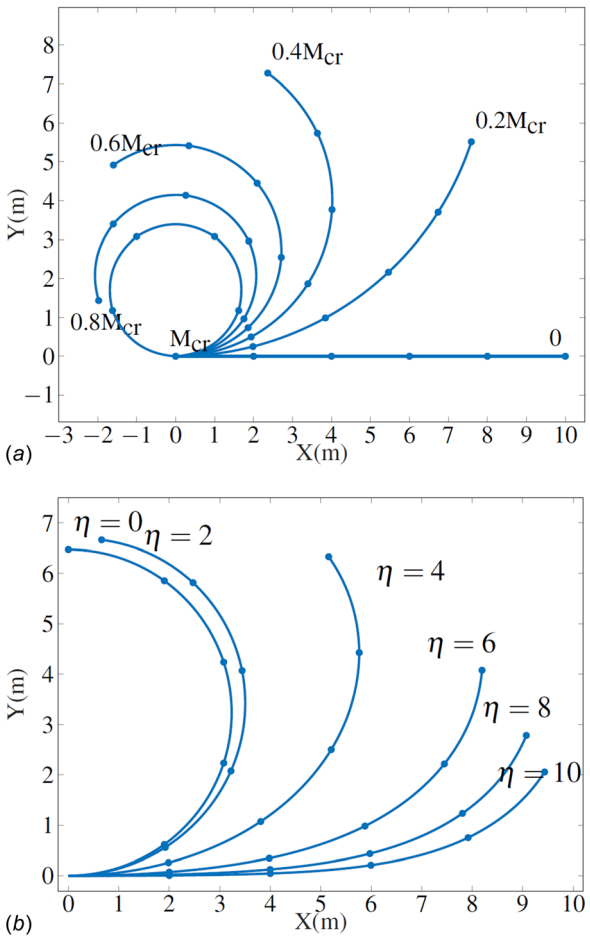

Fig. 2 Static large deformation analysis: (*a*) Cantilever beam under different tip moment (0, $0.2M_{\text{cr}}$, $0.4M_{\text{cr}}$, $0.6M_{\text{cr}}$, $0.8M_{\text{cr}}$, and M_{cr}) and (*b*) rolled-up rotating cantilever beam with different spin speed ($\eta = 0, 2, 4, 6, 8, 10$)

$$\mathbf{f}_I(\ddot{\mathbf{q}} = 0, \dot{\mathbf{q}} = 0, \mathbf{q}_\Omega) + \mathbf{f}_E(\mathbf{q}_\Omega) = \mathbf{p} \tag{26}$$

The results are shown in Fig. 2(*b*) for different dimensionless spin speeds ($\eta = 0, 2, 4, 6, 8, 10$, with $\eta = \sqrt{\rho AL_0^4\Omega^2/EI_z}$). Under the combination of centrifugal force and tip-end moment, the beam is stiffened and has smaller deflection when spin speeds increases. To the authors' knowledge, this kind of analysis (a rotating beam subjected to large deformation by a static tip moment) cannot be found in the literature and qualitative comparison with previous research is impossible.

7 Modal Analysis

Numerical applications in Sec. 6 demonstrate that the proposed C-R model can accurately simulate large deformation in statics. Next, we perform a modal analysis for different constant spin speeds around the prestressed state. The static deformation q_Ω due to centrifugal force is calculated by solving Eq. (26). Substituting the initial deformation q_Ω into Eq. (24) gives the eigenvalue problem related to Eq. (25) with the matrices

$$\tilde{\mathbf{M}}_\Omega = \sum_{i=1}^{4} \mathbf{M}_d^{(i)}(\mathbf{q}_\Omega) \quad \tilde{\mathbf{C}}_\Omega = \sum_{i=1}^{4} \mathbf{C}_d^{(i)}(\mathbf{q}_\Omega)$$

$$\tilde{\mathbf{K}}_\Omega = \mathbf{K}_e(\mathbf{q}_\Omega) + \sum_{i=1}^{4} \mathbf{K}_d^{(i)}(\mathbf{q}_\Omega) \tag{27}$$

The dimensionless natural frequencies $\gamma = \omega\sqrt{\rho AL_0^4/EI_z}$ obtained after simulation are presented in Table 2.

They are in good agreement with published results [17,18]. The difference percentage is less than 0.1% using 5 C-R elements for the first three modes. Figure 3 illustrates the normalized ratio (the ratio between the natural frequency obtained via the proposed model and the one used as Ref. [18]) as a function of the number of elements, for different modes and different spin speeds. The large centrifugal-stressed deformation is successfully taken into consideration and the C-R formulation solution converges to analytical Refs. [17 and 18] whatever the spin speeds.

8 Transient Analysis

In the next simulation, the beam is subjected to a sinusoidal tip force $\mathbf{p} = F_0 \sin(\omega_e t)\mathbf{Y}$. F_0 is equal to 10 MN, and the excitation frequency is $\omega_e = 50\,\text{rad/s}$. The forcing amplitude is chosen very high so as to create a very large amplitude of vibration. The spin speed is zero.

As shown in Figs. 4(*a*) and 4(*b*), a good consistency is obtained between the reference solutions (ANSYS simulation with 50 BEAM189 elements—elements based on total-Lagrangian (T-L) formulation) and the proposed model (only 5 C-R elements). Our

Table 2 Dimensionless frequencies γ under different spin speeds

η		First mode	Second mode	Third mode
0	Proposed model	3.51600	22.03450	61.69720
	Ref. [17]	3.51602	22.03449	61.69721
	Ref. [18]	3.51602	22.03480	61.70490
2	Proposed model	4.13730	22.61490	62.27320
	Ref. [17]	4.13732	22.61492	62.27318
	Ref. [18]	4.13733	22.61530	62.28080
4	Proposed model	5.58500	24.27340	63.96680
	Ref. [17]	5.58500	24.27335	63.96676
	Ref. [18]	5.58503	24.27370	63.97420
8	Proposed model	9.25680	29.99540	70.29300
	Ref. [17]	9.25684	29.99532	70.29296
	Ref. [18]	9.25694	29.99590	70.30020

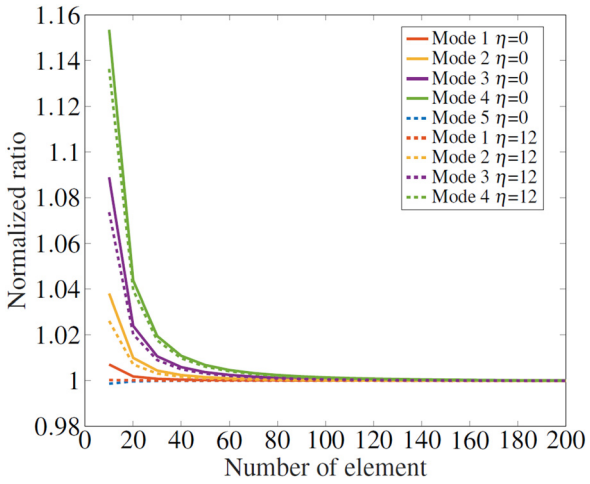

Fig. 3 Convergence analysis for C-R formulation

approach offers a reduction by ten of the number of elements for a similar precision on a very large amplitude of vibration and with a substantial time saving (proposed model: 69 s, ANSYS simulation: 180 s).

9 Response After an Impulsive Force

In addition to a harmonic forcing, another interesting source of excitation is short duration impact pulses. A practical example in turbomachinery application is the debris ingestion. In this section, the impulse excitation on a rotating beam is analyzed using the proposed approach. The impulsive force occurs at $t = 1$ s and has the form of a half sine with a 0.005 s period and 10 MN amplitude. It is applied on the free-end of the beam. The vertical tip displacement responses under three different spin speeds are shown in Fig. 5. When spin speed increases, spin-stiffening effects reduce the amplitude of vibration.

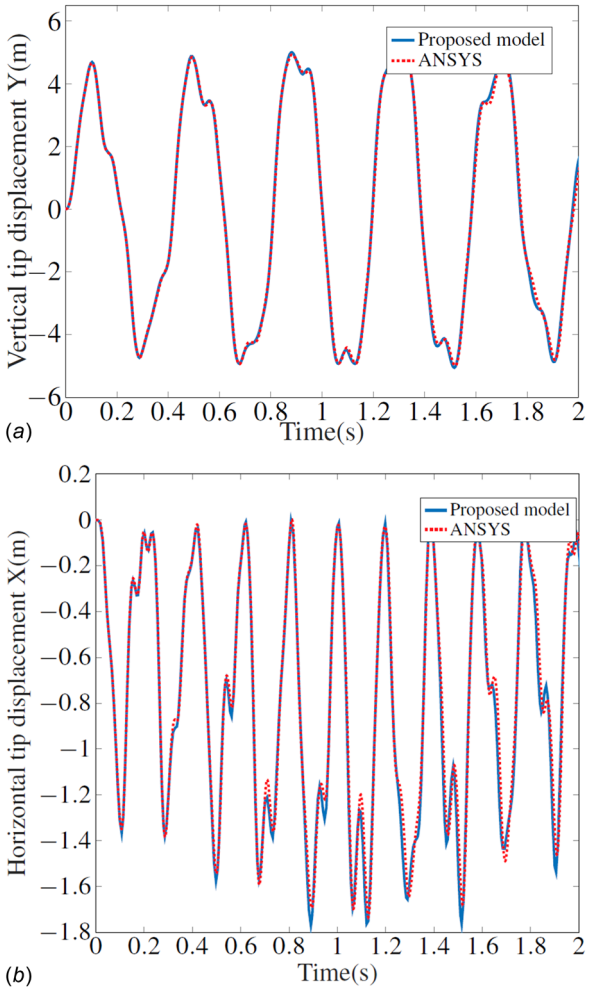

Fig. 4 Large amplitude vibration of cantilever beam: (*a*) vertical displacement and (*b*) horizontal displacement

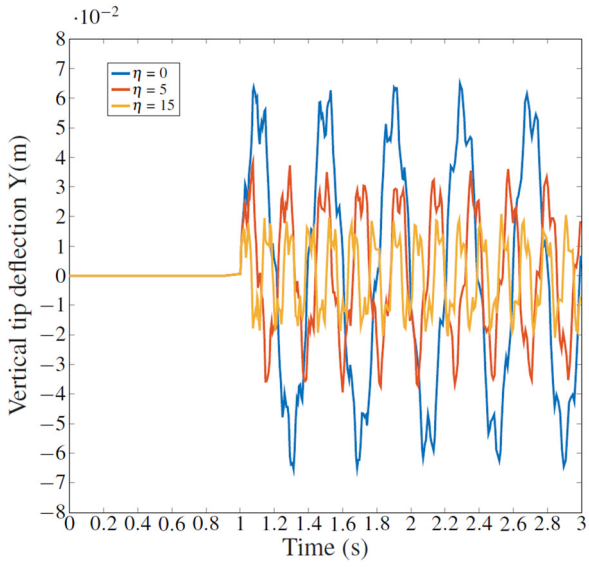

Fig. 5 Vertical tip response to an impulsive force

10 Conclusion

A Co-Rotational finite element model for a rotating beam is proposed. The full nonlinear equations of motion are derived analytically. It was demonstrated that the proposed model can simulate very large static deformations using a small number of elements. The computation time efficiency and accuracy of the approach were proved by comparison with reference solutions (literature and commercial FE software) for very large amplitude vibrations. Besides, the large initial deformations coming from the centrifugal force are correctly taken into account and this has been verified by performing modal analysis for different spin speeds. The proposed C-R rotating beam model is able to simulate the dynamics of turbomachines in the geometrical nonlinear configuration, be it for static, modal, or transient analysis in the event of accidental condition. In this contribution, the proposed method is limited to planar motion in a rotating reference frame. One may consider in further work to construct the three-dimensional C-R rotating beam model.

Appendix A: Differentiation Expressions

The following differentiation relationships can be obtained with Eqs. (7) and (8):

$$\delta\theta = \frac{\mathbf{z}^{\mathrm{T}}}{L_n}\delta\mathbf{q} \qquad \delta\mathbf{b}_2 = \delta\mathbf{b}_3 = \frac{\mathbf{r}\mathbf{z}^{\mathrm{T}} + \mathbf{z}\mathbf{r}^{\mathrm{T}}}{L_n^2}\delta\mathbf{q}$$
$$\delta\left(\frac{\mathbf{z}^{\mathrm{T}}}{L_n}\right) = -\frac{\mathbf{r}\mathbf{z}^{\mathrm{T}} + \mathbf{z}\mathbf{r}^{\mathrm{T}}}{L_n^2}\delta\mathbf{q} \tag{A1}$$

where

$$\mathbf{r} = \begin{bmatrix} -\cos\theta & -\sin\theta & 0 & \cos\theta & \sin\theta & 0 \end{bmatrix}^{\mathrm{T}}$$
$$\mathbf{z} = \begin{bmatrix} \sin\theta & -\cos\theta & 0 & -\sin\theta & \cos\theta & 0 \end{bmatrix}^{\mathrm{T}} \tag{A2}$$

Besides, another important differentiation relation on the rigid body rotation matrix is

$$\frac{\partial}{\partial\theta}\mathbf{T}=\begin{bmatrix}\mathbf{D}&0\\0&\mathbf{D}\end{bmatrix}\mathbf{T}=\mathbf{D}_\theta\mathbf{T}\qquad\mathbf{D}=\begin{bmatrix}0&1&0\\-1&0&0\\0&0&0\end{bmatrix}\tag{A3}$$

Appendix B: Details on the Formulation of the Beam Dynamics

The total kinetic energy, written in Eq. (20), is the sum of five terms. The derivation of each term of this energy is given next. The last term E_{cte} of the total kinetic energy is constant so has no contribution in the Lagrange's equation.

B.1 Quadratic Terms in Global Velocity

The first part of the kinetic energy which contains quadratic terms in velocity is

$$E_c^{(1)}=\frac{1}{2}\dot{\mathbf{q}}^{\mathrm{T}}\mathbf{T}^{\mathrm{T}}\mathbf{M}_l\mathbf{T}\dot{\mathbf{q}}\tag{B1}$$

where $\mathbf{M}_l$ is the local co-rotated mass matrix and $\mathbf{T}$ is the rigid body rotation matrix

$$\mathbf{T}=\begin{bmatrix}\mathbf{T}_g&\mathbf{0}\\\mathbf{0}&\mathbf{T}_g\end{bmatrix},\quad\mathbf{T}_g=\begin{bmatrix}\cos\theta&\sin\theta&0\\-\sin\theta&\cos\theta&0\\0&0&1\end{bmatrix}\tag{B2}$$

$\mathbf{M}_l$ can further be divided into the constant local co-rotated mass matrix $\mathbf{M}^l_{cte}$ which contains constant values and the nonlinear geometrical local mass matrix $\mathbf{M}^l_{\mathrm{NL}}$ which is function of $\bar{\Phi}_I$ and $\bar{\Phi}_I$

$$\mathbf{M}_l=\mathbf{M}^l_{cte}+\mathbf{M}^l_{\mathrm{NL}}\tag{B3}$$

where the local co-rotated mass matrix is given by

$$\mathbf{M}^l_{cte}=\begin{bmatrix}M^{(1)}_{cte}&0&0&M^{(1)}_{cte}/2&0&0\\&M^{(2)}_{cte}&M^{(3)}_{cte}&0&M^{(4)}_{cte}&M^{(5)}_{cte}\\&&M^{(6)}_{cte}&0&-M^{(5)}_{cte}&M^{(7)}_{cte}\\&&&M^{(1)}_{cte}&0&0\\&&&&M^{(2)}_{cte}&-M^{(3)}_{cte}\\\textit{sym.}&&&&&M^{(6)}_{cte}\end{bmatrix}\tag{B4}$$

and

$$\begin{aligned}M^{(1)}_{cte}&=\rho AL_0/3\\M^{(2)}_{cte}&=\rho AL_0 13/35+\rho I_z 6/(5L_0)\\M^{(3)}_{cte}&=\rho AL_0^2 11/210-\rho I_z/10\\M^{(4)}_{cte}&=\rho AL_0 9/70-\rho I_z 6/(5L_0)\\M^{(5)}_{cte}&=-\rho AL_0^2 13/420+\rho I_z/10\\M^{(6)}_{cte}&=\rho AL_0^3/105+\rho I_z L_0 14/105\\M^{(7)}_{cte}&=-\rho AL_0^3/140-\rho I_z L_0/30\end{aligned}$$

and the nonlinear geometrical local mass matrix $\mathbf{M}^l_{\mathrm{NL}}$ is given by

$$\mathbf{M}^l_{\mathrm{NL}}=\begin{bmatrix}0&M^{(1)}_{\mathrm{NL}}&0&0&-M^{(1)}_{\mathrm{NL}}&0\\&M^{(2)}_{\mathrm{NL}}&0&M^{(3)}_{\mathrm{NL}}&-M^{(2)}_{\mathrm{NL}}&0\\&&0&0&0&0\\&&&0&-M^{(3)}_{\mathrm{NL}}&0\\&&&&M^{(2)}_{\mathrm{NL}}&0\\\textit{sym.}&&&&&0\end{bmatrix}\tag{B5}$$

where

$$\begin{aligned}M^{(1)}_{\mathrm{NL}}&=\rho AL_0\left(\bar{\Phi}_I/20-\bar{\Phi}_J/30\right)\\M^{(2)}_{\mathrm{NL}}&=\rho AL_0\left(\bar{\Phi}_I^2/105+\bar{\Phi}_J^2/105-\bar{\Phi}_I\bar{\Phi}_J/70\right)\\&\quad+\rho I_z/L_0\left(2\bar{\Phi}_I^2/15+2\bar{\Phi}_J^2/15-\bar{\Phi}_I\bar{\Phi}_I/15\right)\\M^{(3)}_{\mathrm{NL}}&=\rho AL_0\left(\bar{\Phi}_I/30-\bar{\Phi}_J/20\right)\end{aligned}$$

The local co-rotated mass matrix $\mathbf{M}^l_{cte}$ is equivalent to the mass matrix of linear Rayleigh beam [19] element in which the Euler–Bernoulli hypothesis [20] is considered. The general mass matrix $\mathbf{M}$ is function of θ, $\bar{\Phi}_I$, and $\bar{\Phi}_J$. Hereafter, Lagrange's equation is applied to obtain the corresponding internal inertial force vector

$$\mathbf{f}_I^{(1)}=\mathbf{f}_I^{(11)}+\mathbf{f}_I^{(12)}\tag{B6}$$

The first part of the right-hand side of Eq. (B6) is given as

$$\begin{aligned}\mathbf{f}_I^{(11)}&=\frac{\mathrm{d}}{\mathrm{d}t}\left(\frac{\partial E_c^{(1)}}{\partial\dot{\mathbf{q}}}\right)=\mathbf{M}\ddot{\mathbf{q}}+\frac{\mathrm{d}}{\mathrm{d}t}\left(\mathbf{T}^{\mathrm{T}}\mathbf{M}_l\mathbf{T}\right)\\\dot{\mathbf{q}}&=\frac{\mathrm{d}}{\mathrm{d}t}\left(\mathbf{T}^{\mathrm{T}}\mathbf{M}_l\mathbf{T}\right)=\mathbf{M}\ddot{\mathbf{q}}+\frac{\partial\mathbf{M}}{\partial\theta}\frac{\mathrm{d}\theta}{\mathrm{d}t}+\frac{\partial\mathbf{M}}{\partial\bar{\Phi}_I}\frac{\mathrm{d}\bar{\Phi}_I}{\mathrm{d}t}+\frac{\partial\mathbf{M}}{\partial\bar{\Phi}_J}\frac{\mathrm{d}\bar{\Phi}_J}{\mathrm{d}t}\end{aligned}\tag{B7}$$

Using Eqs. (8) and (A3) (in Appendix A) into Eq. (B7) gives

$$\begin{aligned}&\frac{\partial\mathbf{M}}{\partial\theta}\frac{\mathrm{d}\theta}{\mathrm{d}t}=\mathbf{M}_\theta\left(\frac{\mathbf{z}^{\mathrm{T}}}{L_n}\dot{\mathbf{q}}\right)\quad\frac{\partial\mathbf{M}}{\partial\bar{\Phi}_I}\frac{\mathrm{d}\bar{\Phi}_I}{\mathrm{d}t}=\mathbf{M}_{\bar{\Phi}_I}(\mathbf{b}_2\dot{\mathbf{q}})\\&\frac{\partial\mathbf{M}}{\partial\bar{\Phi}_J}\frac{\mathrm{d}\bar{\Phi}_J}{\mathrm{d}t}=\mathbf{M}_{\bar{\Phi}_J}(\mathbf{b}_3\dot{\mathbf{q}})\end{aligned}\tag{B8}$$

Thus, the expression of $\mathbf{f}_I^{(11)}$ is given by

$$\mathbf{f}_I^{(11)}=\mathbf{M}\ddot{\mathbf{q}}+\left[\mathbf{M}_\theta\left(\frac{\mathbf{z}^{\mathrm{T}}}{L_n}\dot{\mathbf{q}}\right)+\mathbf{M}_{\bar{\Phi}_I}(\mathbf{b}_2\dot{\mathbf{q}})+\mathbf{M}_{\bar{\Phi}_J}(\mathbf{b}_3\dot{\mathbf{q}})\right]\dot{\mathbf{q}}\tag{B9}$$

The second part of the right-hand side of Eq. (B6) is first expressed as

$$\mathbf{f}_I^{(12)}=-\frac{\partial E_c^{(1)}}{\partial\mathbf{q}}=-\left[\frac{\partial E_c^{(1)}}{\partial\theta}\frac{\partial\theta}{\partial\mathbf{q}}+\frac{\partial E_c^{(1)}}{\partial\bar{\Phi}_I}\frac{\partial\bar{\Phi}_I}{\partial\mathbf{q}}+\frac{\partial E_c^{(1)}}{\partial\bar{\Phi}_J}\frac{\partial\bar{\Phi}_J}{\partial\mathbf{q}}\right]\tag{B10}$$

In a similar manner, using Eqs. (8) and (B3) into Eq. (B10) gives

$$\begin{aligned}&\frac{\partial E_c^{(1)}}{\partial\theta}\frac{\partial\theta}{\partial\mathbf{q}}=\frac{1}{2}\dot{\mathbf{q}}^{\mathrm{T}}\mathbf{M}_\theta\dot{\mathbf{q}}\left(\frac{\mathbf{z}}{L_n}\right)\quad\frac{\partial E_c^{(1)}}{\partial\bar{\Phi}_I}\frac{\partial\bar{\Phi}_I}{\partial\mathbf{q}}=\frac{1}{2}\dot{\mathbf{q}}^{\mathrm{T}}\mathbf{M}_{\bar{\Phi}_I}\dot{\mathbf{q}}\left(\mathbf{b}_2^{\mathrm{T}}\right)\\&\frac{\partial E_c^{(1)}}{\partial\bar{\Phi}_J}\frac{\partial\bar{\Phi}_J}{\partial\mathbf{q}}=\frac{1}{2}\dot{\mathbf{q}}^{\mathrm{T}}\mathbf{M}_{\bar{\Phi}_J}\dot{\mathbf{q}}\left(\mathbf{b}_3^{\mathrm{T}}\right)\end{aligned}\tag{B11}$$

Hence, the total inertial force vector for $E_c^{(1)}$ can be written as

$$\mathbf{f}_I^{(1)} = \mathbf{M}\ddot{\mathbf{q}} + \left[\mathbf{M}_\theta\left(\frac{\mathbf{z}^{\mathrm{T}}}{L_n}\dot{\mathbf{q}}\right) + \mathbf{M}_{\bar{\Phi}_I}(\mathbf{b}_2\dot{\mathbf{q}}) + \mathbf{M}_{\bar{\Phi}_J}(\mathbf{b}_3\dot{\mathbf{q}})\right]\dot{\mathbf{q}} - \left[\frac{1}{2}\dot{\mathbf{q}}^{\mathrm{T}}\mathbf{M}_\theta\dot{\mathbf{q}}\left(\frac{\mathbf{z}}{L_n}\right) + \frac{1}{2}\dot{\mathbf{q}}^{\mathrm{T}}\mathbf{M}_{\bar{\Phi}_I}\dot{\mathbf{q}}\left(\mathbf{b}_2^{\mathrm{T}}\right) + \frac{1}{2}\dot{\mathbf{q}}^{\mathrm{T}}\mathbf{M}_{\bar{\Phi}_J}\dot{\mathbf{q}}\left(\mathbf{b}_2^{\mathrm{T}}\right)\right] \tag{B12}$$

With the earlier expression of $\mathbf{f}_I^{(1)}$ and Eq. (22), it is possible to derive analytically the expression of its corresponding tangent dynamic matrices. First, mass matrix can be easily given as $\mathbf{M}_d^{(1)} = \partial\mathbf{f}_I^{(1)}/\partial\ddot{\mathbf{q}} = \mathbf{M}$, and subsequently, the gyroscopic matrix is given as

$$\begin{aligned}\mathbf{C}_d^{(1)} = \frac{\partial\mathbf{f}_I^{(1)}}{\partial\dot{\mathbf{q}}} &= \left[\mathbf{M}_\theta\left(\frac{\mathbf{z}^{\mathrm{T}}}{L_n}\dot{\mathbf{q}}\right) + \mathbf{M}_{\bar{\Phi}_I}(\mathbf{b}_2\dot{\mathbf{q}}) + \mathbf{M}_{\bar{\Phi}_J}(\mathbf{b}_3\dot{\mathbf{q}})\right] \\ &+ \left[\mathbf{M}_\theta\left(\dot{\mathbf{q}}\frac{\mathbf{z}^{\mathrm{T}}}{L_n}\right) + \mathbf{M}_{\bar{\Phi}_I}(\dot{\mathbf{q}}\mathbf{b}_2) + \mathbf{M}_{\bar{\Phi}_J}(\dot{\mathbf{q}}\mathbf{b}_3)\right] \\ &- \left[\left(\frac{\mathbf{z}}{L_n}\dot{\mathbf{q}}^{\mathrm{T}}\right)\mathbf{M}_\theta + \left(\mathbf{b}_2^{\mathrm{T}}\dot{\mathbf{q}}^{\mathrm{T}}\right)\mathbf{M}_{\bar{\Phi}_I} + \left(\mathbf{b}_3^{\mathrm{T}}\dot{\mathbf{q}}^{\mathrm{T}}\right)\mathbf{M}_{\bar{\Phi}_J}\right]\end{aligned} \tag{B13}$$

At last, the tangent dynamic stiffness matrix associated with the first term of the kinetic energy is obtained as

$$\begin{aligned}\mathbf{K}_d^{(1)} &= \mathbf{M}_\theta\ddot{\mathbf{q}}\frac{\mathbf{z}^{\mathrm{T}}}{L_n} + \mathbf{M}_{\bar{\Phi}_I}\ddot{\mathbf{q}}\mathbf{b}_2 + \mathbf{M}_{\bar{\Phi}_J}\ddot{\mathbf{q}}\mathbf{b}_3 \\ &+ \begin{bmatrix}\frac{\mathbf{z}^{\mathrm{T}}}{L_n}\dot{\mathbf{q}}\mathbf{I}_6 & \mathbf{b}_2\dot{\mathbf{q}}\mathbf{I}_6 & \mathbf{b}_3\dot{\mathbf{q}}\mathbf{I}_6\end{bmatrix}\begin{bmatrix}\frac{\partial\mathbf{M}_\theta}{\partial\theta} & \frac{\partial\mathbf{M}_\theta}{\partial\bar{\Phi}_I} & \frac{\partial\mathbf{M}_\theta}{\partial\bar{\Phi}_J} \\ \frac{\partial\mathbf{M}_{\bar{\Phi}_I}}{\partial\theta} & \frac{\partial\mathbf{M}_{\bar{\Phi}_I}}{\partial\bar{\Phi}_I} & \frac{\partial\mathbf{M}_{\bar{\Phi}_I}}{\partial\bar{\Phi}_J} \\ \frac{\partial\mathbf{M}_{\bar{\Phi}_J}}{\partial\theta} & \frac{\partial\mathbf{M}_{\bar{\Phi}_J}}{\partial\bar{\Phi}_I} & \frac{\partial\mathbf{M}_{\bar{\Phi}_J}}{\partial\bar{\Phi}_J}\end{bmatrix} \\ &\times \begin{bmatrix}\dot{\mathbf{q}}\frac{\mathbf{z}^{\mathrm{T}}}{L_n} \\ \dot{\mathbf{q}}\mathbf{b}_2 \\ \dot{\mathbf{q}}\mathbf{b}_3\end{bmatrix} - \frac{1}{2}\begin{bmatrix}\dot{\mathbf{q}}^{\mathrm{T}}\frac{\mathbf{z}}{L_n} & \dot{\mathbf{q}}^{\mathrm{T}}\mathbf{b}_2^{\mathrm{T}} & \dot{\mathbf{q}}^{\mathrm{T}}\mathbf{b}_3^{\mathrm{T}}\end{bmatrix} \\ &\times \begin{bmatrix}\frac{\partial\mathbf{M}_\theta}{\partial\theta} & \frac{\partial\mathbf{M}_\theta}{\partial\bar{\Phi}_I} & \frac{\partial\mathbf{M}_\theta}{\partial\bar{\Phi}_J} \\ \frac{\partial\mathbf{M}_{\bar{\Phi}_I}}{\partial\theta} & \frac{\partial\mathbf{M}_{\bar{\Phi}_I}}{\partial\bar{\Phi}_I} & \frac{\partial\mathbf{M}_{\bar{\Phi}_I}}{\partial\bar{\Phi}_J} \\ \frac{\partial\mathbf{M}_{\bar{\Phi}_J}}{\partial\theta} & \frac{\partial\mathbf{M}_{\bar{\Phi}_J}}{\partial\bar{\Phi}_I} & \frac{\partial\mathbf{M}_{\bar{\Phi}_J}}{\partial\bar{\Phi}_J}\end{bmatrix}\begin{bmatrix}\dot{\mathbf{q}}\frac{\mathbf{z}^{\mathrm{T}}}{L_n} \\ \dot{\mathbf{q}}\mathbf{b}_2 \\ \dot{\mathbf{q}}\mathbf{b}_3\end{bmatrix} \\ &+ \left(\mathbf{M}_{\bar{\Phi}_I} + \mathbf{M}_{\bar{\Phi}_J} - \mathbf{M}_\theta\right)\dot{\mathbf{q}}\dot{\mathbf{q}}^{\mathrm{T}}\frac{\mathbf{r}\mathbf{z}^{\mathrm{T}} + \mathbf{z}\mathbf{r}^{\mathrm{T}}}{L_n^2} \\ &- \frac{1}{2}\dot{\mathbf{q}}^{\mathrm{T}}\left(\mathbf{M}_{\bar{\Phi}_I} + \mathbf{M}_{\bar{\Phi}_J} - \mathbf{M}_\theta\right)\dot{\mathbf{q}}\frac{\mathbf{r}\mathbf{z}^{\mathrm{T}} + \mathbf{z}\mathbf{r}^{\mathrm{T}}}{L_n^2}\end{aligned} \tag{B14}$$

where $\mathbf{I}_6$ is a 6×6 identity matrix.

B.2 Quadratic Terms in Global Displacement

The second part of the kinetic energy contains the quadratic terms in global displacement. It is explicitly written as

$$E_c^{(2)} = \frac{1}{2}\mathbf{q}^{\mathrm{T}}\mathbf{K}_\Omega\mathbf{q} \quad \mathbf{K}_\Omega = \Omega^2\frac{\rho AL_0}{6}\begin{bmatrix}2&0&0&1&0&0\\0&0&0&0&0&0\\0&0&0&0&0&0\\1&0&0&2&0&0\\0&0&0&0&0&0\\0&0&0&0&0&0\end{bmatrix} \tag{B15}$$

The corresponding internal inertial force vector obtained from Lagrange's equation is given by

$$\mathbf{f}_I^{(2)} = \frac{\mathrm{d}}{\mathrm{d}t}\left(\frac{\partial E_c^{(2)}}{\partial\dot{\mathbf{q}}}\right) - \frac{\partial E_c^{(2)}}{\partial\mathbf{q}} = -\mathbf{K}_\Omega\mathbf{q} \tag{B16}$$

Thus, the relevant tangent dynamic matrices can be formulated as $\mathbf{M}_d^{(2)} = \partial\mathbf{f}_I^{(2)}/\partial\ddot{\mathbf{q}} = \mathbf{0}$, $\mathbf{C}_d^{(2)} = \partial\mathbf{f}_I^{(2)}/\partial\dot{\mathbf{q}} = \mathbf{0}$ and $\mathbf{K}_d^{(2)} = \partial\mathbf{f}_I^{(2)}/\partial\mathbf{q} = -\mathbf{K}_\Omega$.

B.3 Linear Terms in Global Displacement

The third part of kinetic energy gathers the first-order global displacement vector

$$E_c^{(3)} = \mathbf{F}_\Omega^{\mathrm{T}}\mathbf{q} \quad \mathbf{F}_\Omega = \frac{\Omega^2\rho AL_0}{60}\begin{bmatrix}F_{\Omega,1} & 0 & 0 & F_{\Omega,2} & 0 & 0\end{bmatrix}^{\mathrm{T}} \tag{B17}$$

where $\mathbf{F}_\Omega$ is function of θ, $\bar{\Phi}_I$, and $\bar{\Phi}_J$

$$\begin{aligned}F_{\Omega,1} &= 10(2X_I + X_J) + L_0\sin\theta(2\bar{\Phi}_J - 3\bar{\Phi}_J) \\ F_{\Omega,2} &= 10(X_I + 2X_J) + L_0\sin\theta(3\bar{\Phi}_J - 2\bar{\Phi}_J)\end{aligned} \tag{B18}$$

Thus, the inertial force vector is given by

$$\mathbf{f}_I^{(3)} = \frac{\mathrm{d}}{\mathrm{d}t}\left(\frac{\partial E_c^{(3)}}{\partial\dot{\mathbf{q}}}\right) - \frac{\partial E_c^{(3)}}{\partial\mathbf{q}} = -\mathbf{F}_\Omega - \mathbf{q}^{\mathrm{T}}\left(\mathbf{F}_\Omega^\theta\frac{\mathbf{z}}{L_n} + \mathbf{F}_\Omega^{\bar{\Phi}_I}\mathbf{b}_2^{\mathrm{T}} + \mathbf{F}_\Omega^{\bar{\Phi}_J}\mathbf{b}_3^{\mathrm{T}}\right) \tag{B19}$$

Subsequently, the corresponding tangent dynamic matrices are $\mathbf{M}_d^{(3)} = \partial\mathbf{f}_I^{(3)}/\partial\ddot{\mathbf{q}} = \mathbf{0}$, $\mathbf{C}_d^{(3)} = \partial\mathbf{f}_I^{(3)}/\partial\dot{\mathbf{q}} = \mathbf{0}$ and

$$\mathbf{K}_d^{(3)} = \frac{\partial\mathbf{f}_I^{(4)}}{\partial\mathbf{q}} - \begin{bmatrix}\frac{\mathbf{z}}{L_n} & \mathbf{b}_2^{\mathrm{T}} & \mathbf{b}_3^{\mathrm{T}}\end{bmatrix}\begin{bmatrix}\mathbf{q}^{\mathrm{T}}\frac{\partial\mathbf{F}_\Omega^\theta}{\partial\theta} & \mathbf{q}^{\mathrm{T}}\frac{\partial\mathbf{F}_\Omega^\theta}{\partial\bar{\Phi}_I} & \mathbf{q}^{\mathrm{T}}\frac{\partial\mathbf{F}_\Omega^\theta}{\partial\bar{\Phi}_J} \\ \mathbf{q}^{\mathrm{T}}\frac{\partial\mathbf{F}_\Omega^{\bar{\Phi}_I}}{\partial\theta} & \mathbf{q}^{\mathrm{T}}\frac{\partial\mathbf{F}_\Omega^{\bar{\Phi}_I}}{\partial\bar{\Phi}_I} & \mathbf{q}^{\mathrm{T}}\frac{\partial\mathbf{F}_\Omega^{\bar{\Phi}_I}}{\partial\bar{\Phi}_J} \\ \mathbf{q}^{\mathrm{T}}\frac{\partial\mathbf{F}_\Omega^{\bar{\Phi}_J}}{\partial\theta} & \mathbf{q}^{\mathrm{T}}\frac{\partial\mathbf{F}_\Omega^{\bar{\Phi}_J}}{\partial\bar{\Phi}_I} & \mathbf{q}^{\mathrm{T}}\frac{\partial\mathbf{F}_\Omega^{\bar{\Phi}_J}}{\partial\bar{\Phi}_J}\end{bmatrix}\begin{bmatrix}\frac{\mathbf{z}^{\mathrm{T}}}{L_n} \\ \mathbf{b}_2 \\ \mathbf{b}_3\end{bmatrix} \tag{B20}$$

B.4 Zero-Order Terms in Global Displacement and Velocity

The term E_{NL} of the kinetic energy (20) is function of local displacement vector $\bar{\mathbf{q}}$ only, while the last term E_{cte} is constant. E_{NL} is given by

$$\begin{aligned}E_{NL} &= \Omega^2\rho I_z L_0\sin^2\theta/2 - \Omega^2\rho L_0^2 AX_I\sin\theta\bar{\Phi}_I/20 \\ &+ \Omega^2\rho L_0^2 AX_J\sin\theta\bar{\Phi}_J/30 - \Omega^2\rho L_0^2 AX_I\sin\theta\bar{\Phi}_I/30 \\ &+ \Omega^2\rho L_0^2 AX_J\sin\theta\bar{\Phi}_I/20 + \Omega^2\rho I_z L_0\bar{\Phi}_I^2/15 \\ &+ \Omega^2\rho I_z L_0\bar{\Phi}_J^2/15 + \Omega^2\rho L_0^3 A\bar{\Phi}_J^2/210 \\ &+ \Omega^2\rho L_0^3 A\bar{\Phi}_I^2/210 - \Omega^2\rho L_0^3 A\sin\theta\bar{\Phi}_I\bar{\Phi}_J/140 \\ &- \Omega^2\rho I_z L_0\sin^2\theta\bar{\Phi}_I^2/15 - \Omega^2\rho I_z L_0\sin^2\theta\bar{\Phi}_J^2/15 \\ &- \Omega^2\rho I_z L_0\bar{\Phi}_I\bar{\Phi}_J/30 - \Omega^2\rho I_z L_0\sin^2\theta\bar{\Phi}_I\bar{\Phi}_J/30\end{aligned} \tag{B21}$$

The associated internal inertial force vector is

$$\mathbf{f}_I^{(4)} = \frac{\mathrm{d}}{\mathrm{d}t}\left(\frac{\partial E_{\mathrm{NL}}}{\partial\dot{\mathbf{q}}}\right) - \frac{\partial E_{\mathrm{NL}}}{\partial\mathbf{q}} = -E_{\mathrm{NL}}^\theta\frac{\mathbf{z}}{L_n} - E_{\mathrm{NL}}^{\bar{\Phi}_I}\mathbf{b}_2^{\mathrm{T}} - E_{\mathrm{NL}}^{\bar{\Phi}_I}\mathbf{b}_3^{\mathrm{T}} \tag{B22}$$

Subsequently, the related tangent dynamic matrices are $\mathbf{M}_d^{(4)} = \partial \mathbf{f}_I^{(4)} / \partial \ddot{\mathbf{q}} = \mathbf{0}$, $\mathbf{C}_d^{(4)} = \partial \mathbf{f}_I^{(4)} / \partial \dot{\mathbf{q}} = \mathbf{0}$ and

$$\mathbf{K}_d^{(4)} = \frac{\partial \mathbf{f}_I^{(4)}}{\partial \mathbf{q}} = -\left(E_{\mathrm{NL}}^{\bar{\Phi}_I} + E_{\mathrm{NL}}^{\bar{\Phi}_J} - E_{\mathrm{NL}}^{\theta}\right) \frac{\mathbf{r}\mathbf{z}^{\mathrm{T}} + \mathbf{z}\mathbf{r}^{\mathrm{T}}}{L_n^2} - \begin{bmatrix} \dfrac{\mathbf{z}}{L_n} & \mathbf{b}_2^{\mathrm{T}} & \mathbf{b}_3^{\mathrm{T}} \end{bmatrix} \begin{bmatrix} \dfrac{\partial E_{\mathrm{NL}}^{\theta}}{\partial \theta} & \dfrac{\partial E_{\mathrm{NL}}^{\theta}}{\partial \bar{\Phi}_I} & \dfrac{\partial E_{\mathrm{NL}}^{\theta}}{\partial \bar{\Phi}_J} \\ \dfrac{\partial E_{\mathrm{NL}}^{\bar{\Phi}_I}}{\partial \theta} & \dfrac{\partial E_{\mathrm{NL}}^{\bar{\Phi}_I}}{\partial \bar{\Phi}_I} & \dfrac{\partial E_{\mathrm{NL}}^{\bar{\Phi}_I}}{\partial \bar{\Phi}_J} \\ \dfrac{\partial E_{\mathrm{NL}}^{\bar{\Phi}_J}}{\partial \theta} & \dfrac{\partial E_{\mathrm{NL}}^{\bar{\Phi}_J}}{\partial \bar{\Phi}_I} & \dfrac{\partial E_{\mathrm{NL}}^{\bar{\Phi}_J}}{\partial \bar{\Phi}_J} \end{bmatrix} \begin{bmatrix} \dfrac{\mathbf{z}^{\mathrm{T}}}{L_n} \\ \mathbf{b}_2 \\ \mathbf{b}_3 \end{bmatrix} \tag{B23}$$

References

[1] Thomas, O., Sénéchal, A., and Deü, J.-F., 2016, "Hardening/Softening Behavior and Reduced Order Modeling of Nonlinear Vibrations of Rotating Cantilever Beams," Nonlinear Dyn., **86**(2), pp. 1293–1318.

[2] Stoykov, S., and Ribeiro, P., 2013, "Vibration Analysis of Rotating 3D Beams by the p-Version Finite Element Method," Finite Elem. Anal. Des., **65**, pp. 76–88.

[3] Bauchau, O. A., and Hong, C.-H., 1987, "Finite Element Approach to Rotor Blade Modeling," J. Am. Helicopter Soc., **32**(1), pp. 60–67.

[4] Vinod, K., Gopalakrishnan, S., and Ganguli, R., 2007, "Free Vibration and Wave Propagation Analysis of Uniform and Tapered Rotating Beams Using Spectrally Formulated Finite Elements," Int. J. Solids Struct., **44**(18–19), pp. 5875–5893.

[5] Bekhoucha, F., Rechak, S., Duigou, L., and Cadou, J.-M., 2013, "Nonlinear Forced Vibrations of Rotating Anisotropic Beams," Nonlinear Dyn., **74**(4), pp. 1281–1296.

[6] Le, T.-N., Battini, J.-M., and Hjiaj, M., 2011, "Efficient Formulation for Dynamics of Corotational 2D Beams," Comput. Mech., **48**(2), pp. 153–161.

[7] Iura, M., Suetake, Y., and Atluri, S., 2003, "Accuracy of Co-Rotational Formulation for 3-D Timoshenko's Beam," Comput. Model. Eng. Sci., **4**(2), pp. 249–258.

[8] Iura, M., and Atluri, S., 2003, "Advances in Finite Rotations in Structural Mechanics," Comput. Model. Eng. Sci., **4**(2), pp. 213–216.

[9] Felippa, C. A., and Haugen, B., 2005, "A Unified Formulation of Small-Strain Corotational Finite Elements—I: Theory," Comput. Methods Appl. Mech. Eng., **194**(21–24), pp. 2285–2335.

[10] Masashi, I., 1994, "Effects of Coordinate System on the Accuracy of Corotational Formulation for Bernoulli-Euler's Beam," Int. J. Solids Struct., **31**(20), pp. 2793–2806.

[11] Battini, J.-M., 2002, "Co-Rotational Beam Elements in Instability Problems," Ph.D. thesis, KTH, Stockholm, Sweden.

[12] Crisfield, M. A., 1997, *Non-Linear Finite Element Analysis of Solids and Structures, Volume 2: Advanced Topics*, Wiley, Hoboken, NJ.

[13] Simo, J. C., and Vu-Quoc, L., 1986, "A Three-Dimensional Finite-Strain Rod Model—Part II: Computational Aspects," Comput. Methods Appl. Mech. Eng., **58**(1), pp. 79–116.

[14] Dufva, K., Sopanen, J., and Mikkola, A., 2005, "A Two-Dimensional Shear Deformable Beam Element Based on the Absolute Nodal Coordinate Formulation," J. Sound Vib., **280**(3–5), pp. 719–738.

[15] Crisfield, M. A., 1990, "A Consistent Co-Rotational Formulation for Non-Linear, Three-Dimensional, Beam-Elements," Comput. Methods Appl. Mech. Eng., **81**(2), pp. 131–150.

[16] Omar, M., and Shabana, A., 2001, "A Two-Dimensional Shear Deformable Beam for Large Rotation and Deformation Problems," J. Sound Vib., **243**(3), pp. 565–576.

[17] Hodges, D. Y., and Rutkowski, M. Y., 1981, "Free-Vibration Analysis of Rotating Beams by a Variable-Order Finite-Element Method," AIAA J., **19**(11), pp. 1459–1466.

[18] Banerjee, J., 2000, "Free Vibration of Centrifugally Stiffened Uniform and Tapered Beams Using the Dynamic Stiffness Method," J. Sound Vib., **233**(5), pp. 857–875.

[19] Gan, B. S., 2017, *An Isogeometric Approach to Beam Structures: Bridging the Classical to Modern Technique*, Springer, Cham, Switzerland.

[20] Przemieniecki, J. S., 1985, *Theory of Matrix Structural Analysis*, Courier Corporation, North Chelmsford, MA.